Structure–Properties Relations of Thermally Cured Epoxy–Lignin Polyblends

D. FELDMAN,[1,*] D. BANU,[1] A. NATANSOHN,[2] and J. WANG[1]

[1]Centre for Building Studies, Concordia University, Montréal, Québec, Canada H3G 1M8 and [2]Department of Chemistry, Queen's University, Kingston, Ontario, Canada K7L 2N6

SYNOPSIS

A bisphenol A based epoxy adhesive (EP) was modified by polyblending with Kraft Lignin (L). A systematic investigation of the thermally cured EP–L polyblends with up to 40% by weight L was undertaken. Adhesive shear tests, differential scanning calorimetry (DSC), dynamic mechanical analysis (DMA), and solid-state CP-MAS NMR spectroscopy were performed to establish the effect of L on the mechanical properties of the polyblends and on the morphology of these crosslinked structures. The possibility of an enhanced degree of bonding between L and the EP network is discussed. This bonding can arise from a chemical reaction between L and some unreacted amine groups present in the hardener.

INTRODUCTION

In the construction industry, epoxy resins find a variety of applications such as adhesive mortars, composite materials, and coatings. Epoxy polymers show excellent adhesion to the most common metals, glass, ceramics, concrete, and other materials.

Their superior performance is in essence, due to the basic chemical structure of epoxy. Epoxy resins have a very high polarity. The presence of aliphatic hydroxyl and ether groups in the primary resin chain as well as in the cured polymer serve to create an electromagnetic bonding between the epoxy macromolecules and the surface being bonded.[1]

In commercial applications epoxy resins are rarely used without the incorporation of some other materials. Filling or polyblending are both used to enhance their performance by providing additional mechanical properties or modifying the physical characteristics of the blends.

In previous work,[2–4] the curing kinetics and some mechanical and thermal properties of an epoxy–lignin polyblend were investigated.

Lignin was chosen because, first, it is an abundant nontoxic amorphous natural polymer and, second,

it is an inexpensive by-product of the forest industry for which there is, at present, only a small market. However, a combination of the abundance of lignins, their versatility due to the variety of available sources, the recent interest in renewable resources, and the care against the pollution of our environment have opened up research into the potential applications of lignins in many fields.[5]

More and more studies have been dedicated to elucidating its macromolecular structure. Considerable attention has also been devoted to the examination of those properties that make lignins predisposed for use in the reinforcement and modification of plastics.

The basic chemical components of lignin (primarily syringyl, guaiacyl, and p-hydroxy phenol) are bonded together by a set of linkages to form a very complex matrix. This matrix comprises a variety of functional groups, such as hydroxyl, methoxyl, and carbonyl, which impart a high polarity to the lignin macromolecule. Due to these characteristics, lignin appears to be an extremely promising material in the field of organic fillers or as a chemical component in polyblends.

As we have shown elsewhere,[2–4] a bisphenol A based epoxy polymer adhesive (EP) was modified by polyblending with Kraft lignin (L) in amounts of up to 20% by weight.

---

* To whom correspondence should be addressed.

These are different from other EP–L adhesives described in the literature[6-10] because L is not modified chemically. For example, Shirashi et al.[6,7] obtained an EP–L system where L was modified, glycidylated, and cured at 140°C by hot pressing using aliphatic amines as a curing agent. Tomita et al.[8] described a new EP–L adhesive in which L is modified by ozonization. Nieh and Glasser[9] report the synthesis of an epoxide resin on the basis of L by catalytic reaction of epychlorohydrin with hydroxypropyl lignin. The resulting L–epoxide can be crosslinked with aliphatic amine or anhydrides. Cured epoxy had L derivative contents of up to 95%. Ball and co-workers[10] obtained kraft lignin–epoxy resin blends in the melt state at 190°C and cured them with phthalic anhydride at 160°C.

The EP–L polyblends reported in previous studies were prepared by thoroughly hand mixing the EP and L and thereafter cured at room temperature.[3] In amounts between 5 and 20% of these polyblends L had rather a detrimental effect on the adhesive strength (single lap shear using tensile load). An improvement of the adhesive strength shear of both the EP and particularly the EP–L polyblends was obtained after a postcuring process (4 h at 75°C). Differential scanning calorimetry and DMA analysis for 5–20% L in EP–L polyblends disclosed a single T_g, which is characteristic for monophasic systems.[4] The DMA data revealed a gradual reduction of the peak value of tanδ in relation to the amount of L in the polyblends. This was apparent due to an increase in the tensile storage modulus and a decrease of tensile loss modulus at temperatures close to T_g. The behavior of the modulus at or around the T_g of the blends as well as the significant improvement in the adhesion of EP–L polyblends after the postcuring process were explained by a bond between L and the EP network that could develop at higher curing temperatures. Furthermore, the bonding was specifically considered to take place between L and possible unreacted amine groups of the hardener.

Amine cured EP networks are generally assumed to result exclusively from addition reactions of epoxide groups with primary and secondary amines.[11] However, these reactions are often incomplete due to steric and diffusional restrictions, and additional reactions such as epoxide homopolymerization can occur.[11-14] Hence the presence of traces of unreacted amine in the cured EP network is generally accepted.

The results obtained to evaluate the curing kinetics of the same EP–hardener system in the presence of L have shown an interaction between L and the amine hardener.[2] The results obtained from dynamic experiments have shown that the presence of L did not significantly affect the EP curing process. However, a slight increase in activation energy and a slight reduction of the cure rate with a corresponding increase in L content could at a first glance be explained by an interaction between L and the polyamine hardener. This explanation was based on the results of further thermal analysis between L–polyamine hardener and L–EP prepolymer. In the dynamic experiments, conducted between −30 and 200°C and at a heating rate of 10°C/min, an exothermic reaction took place between L and the hardener at ca. 50°C, whereas no interaction could be detected between L and the EP prepolymer.

This article presents the results of further studies performed on EP–L polyblends cured above their T_g. We were interested in the effect of L on the mechanical properties of polyblends and its effect on the morphology of the crosslinked structure after thermal curing. Consequently, the thermal, viscoelastic, and adhesive performance of the EP–L polyblends as a function of L content are discussed and correlated with CP-MAS NMR spectra.

EXPERIMENTAL

Materials

1. An epoxy prepolymer based on DGEBA (Ciba Geigy 1200 CA resin) was used without purification. It was cured with an accelerated polyamine (Ciba Geigy HY 2992). The materials were reacted stoichiometrically, according to their respective equivalent weights, i.e., 1200 CA, 180 g/eq; HY 2992, 55 g/eq. Both resin and hardener are liquid at room temperature.

2. The second polymer, Kraft lignin (L), is chemically extracted from a mixture of hardwoods and precipitated from the black liquor with sulfuric acid and the pH adjusted to about 6–7 (Tomlinite, Domtar). It has the following characteristics:

(a) Molecular weight: weight-averaged molecular weight $(\bar{M}_w)$, 2800; number average molecular weight $(\bar{M}_n)$: 650; polydispersity: $(\bar{M}_w/\bar{M}_n)$: 4.3.

(b) Assays: C: 65.06%; H: 6.03%; S: 1.59%; total OH: 10.7% (including phenolic and aliphatic); methoxyl: 17.2%; carbonyl: 5.0%.

(c) Specific gravity: 1.28 g/cm³.

(d) Glass transition temperature: 132 ± 3°C: (a) determined by gel permeation chromatography (acetylated L); (b) data furnished by Domtar Research Center, Seneville, Quebec; (c) determined according to ASTM D-153; (d) determined by DSC analysis (inflection point) on dried samples.

3. Crystalline silica, Tripoli (Malvern Minerals Co.), with a specific gravity of 2.65 g/cm³ was used as a "control" filler.

4. The substrate material used for the adhesive joints was an aluminum alloy (2024T3 temper) corresponding to ASTM D-1002. Preparation of the bonding surface was well defined and controlled. The aluminum bars were thoroughly degreased with acetone, air dried, etched for 15 min at 65°C with a chromic mixture (sulfuric acid–sodium dichromate solution), washed first with tap water and then with distilled water, after which they were dried at 100°C for 30 min, and finally, stored in a dessicator until used.

Preparation of Cured Samples

The polyblends were prepared by manually stirring the epoxy prepolymer and the corresponding quantity of L (10–40% by weight of polyblend) for 2 min; the equivalent quantity of curing agent was added and the resulting mixture was then stirred for another 5 min.

Twelve minutes after preparation, the mixtures were poured into silicone molds (65 × 12 × 3 mm) for DMA analyses or directly in preweighed aluminum DSC pans then cured in a forced circulation oven at 100°C for 2 h. The cured samples were then allowed to cool in a dessicator. The DSC and DMA tests were performed 7 days after sample preparation.

Another type of sample was prepared for DMA tests by placing the obtained mixture on a strip of fiberglass previously mounted between the horizontal clamps of the DMA. The clamps were set at a standard distance of 10.5 mm before being tightened. The ends of the cloth were wrapped with a layer of aluminum foil (where faces of the clamps were in contact with the sample) to prevent the clamps from adhering to the sample after cure. The thermal program was also set up 12 min after the mixture preparation.

Single lap shear joints fabricated with aluminum substrates (101.6 × 25.4 × 1.6 mm) having an overlap length of 12.7 mm were used to evaluate the adhesive tensile shear strength of the blends.

The mixtures were applied across both sides of the overlap area. Two wires were placed across the bonded area (between the substrates) to ensure a uniform adhesive thickness (0.22 ± 0.03 mm) in all specimens. After curing at the specified temperature for 2 h, the specimens were permitted to cool to room temperature (25°C) in a dessicator for a further 2 h.

Physical Testing and Characterization

The adhesive shear strength by tension loading (ASTM D-1002) was determined using an Instron 1125 universal testing machine at a cross head speed of 2 mm/min and at a testing temperature of 23 ± 2°C. In all cases, the values plotted on the graphs are an average of 5–10 determinations.

The T_g of cured EP and EP–L polyblends was determined on a 910 DuPont differential scanning calorimeter connected with a 1090 DuPont thermal analyzer. Samples were run at a constant heating rate of 20°C/min under a nitrogen atmosphere between −40 and 180°C.

The DMA analyses were performed on a 982 DuPont dynamic mechanical analyzer connected with a 1090 DuPont thermal analyzer at a heating rate of 5°C/min under a nitrogen atmosphere between 20 and 180°C.

For cured samples, vertical clamps were used whereas the horizontal ones were used for uncured samples. Data obtained from both the DSC and DMA analyses are an average of at least three determinations.

Solid-state NMR spectra were obtained on a Bruker CXP-200 spectrometer with a Doty probe.

RESULTS

Adhesive Shear Strength Using Tensile Load

Although the aliphatic amines are generally effective curing agents at room temperature, higher bond strengths can be achieved if heat is used to cure the EP, possibly because of the greater opportunity for the formation of additional crosslinks due to the increased polymer chain flexibility at elevated temperatures.

There are no theoretical methods for calculating optimum cure conditions, but the usual process is to determine the degree of cure experimentally in terms of optimizing the desired properties.[11]

Consequently, a series of EP–L40 polyblends was cured 24 h at room temperature and a subsequent series for 2 h at 75, 100, and 120°C, respectively, and then tested for adhesive shear strength. (Some preliminary DSC tests indicated a T_g for the polyblends in the range of 70–72°C.)

The effect of curing temperature on the adhesive shear strength is shown in Figure 1.

Curing at 75°C, which is slightly above the T_g of the polyblends, improved the adhesive strength significantly, and even better results were obtained for samples cured at 100°C. Above a curing temperature
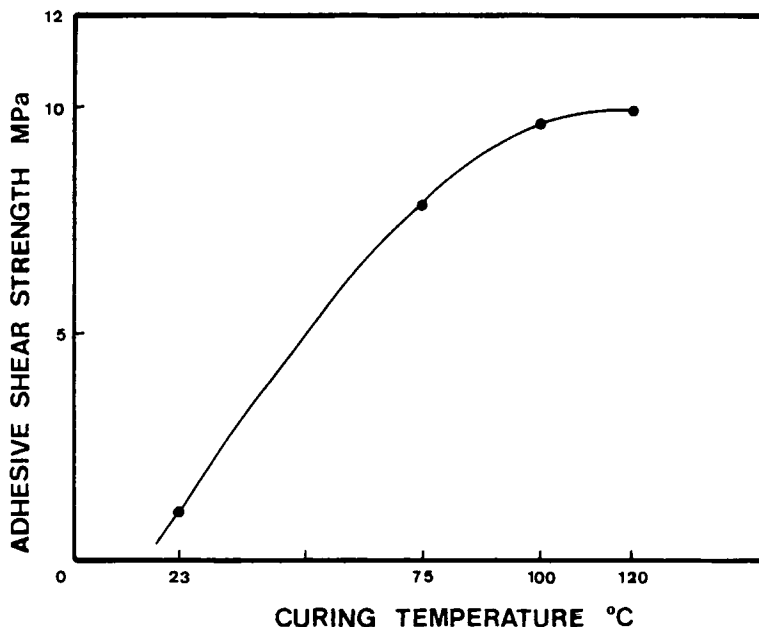
Figure 1   Adhesive shear strength for EP-L40 polyblends vs. curing temperature.

of 100°C there is no increase of adhesive strength, hence a curing temperature of 100°C was considered optimal, and this was the curing mode adopted for thermally cured samples.

The effect of the amount of L on the adhesive shear strength of the thermally cured polyblends is shown in Figure 2. The results shown in Figure 2 are summarized as follows:

1. Failure in all the tests was interfacial, i.e., adhesive.
2. Polyblends with 10, 20, 25, and 30% L showed a considerable improvement in adhesive shear strength in comparison to the control EP (i.e., 53, 78, 39, and 23% higher, respectively).
3. The highest adhesive shear strength occurred at 20% L content.
4. For EP-40L the adhesive shear strength was 16% lower in comparison with the control EP.

For the EP-20L polyblends, which exhibit the highest adhesive shear strength, one may make the following observations:

(i) As can be seen in Figure 2, thermal curing increased the adhesive shear strength of control EP only threefold, whereas it increased that of EP-20L about six times.

(ii) Tensile shear strength for standard cured EP control and EP-20L polyblends was 3.9 and

3.8 MPa, respectively.[3] It appears that the presence of L has a negligible effect on the adhesive shear strength. This is not surprising if one considers the mechanical resistance of L. Young's modulus of L is very low, i.e., 6.6 GPa,[15] in comparison with the modulus of the other ordinary EP fillers (i.e., alumina, 320 GPa; silica, 97 GPa; dolomite, 78 GPa).[16] Moloney and Colab[17] revealed that the modulus and strength of a filler is one of the principal parameters that determine the strength and toughness of a filled epoxide resin. Other cited parameters are the volume fraction of filler, the particle size, the filler aspect ratio, the resin-filler adhesion, and the toughness of the matrix.

These two observations concerning EP-20L polyblends shows that the beneficial effect of L toward the bond strength takes place only at elevated temperatures. In polyblends cured a room temperature L acts only as a filler. Besides comparing the adhesive tensile strength of the EP and EP-20L specimens for either standard or thermally cured samples, we sought also to establish if the presence of L has the same effect toward the adhesive strength when most of the crosslinking process takes place at room temperature.

Consequently, sets of EP control and EP-20L specimens were thermally cured following a scheduled delay of 1, 3, and 7 days after their preparation.
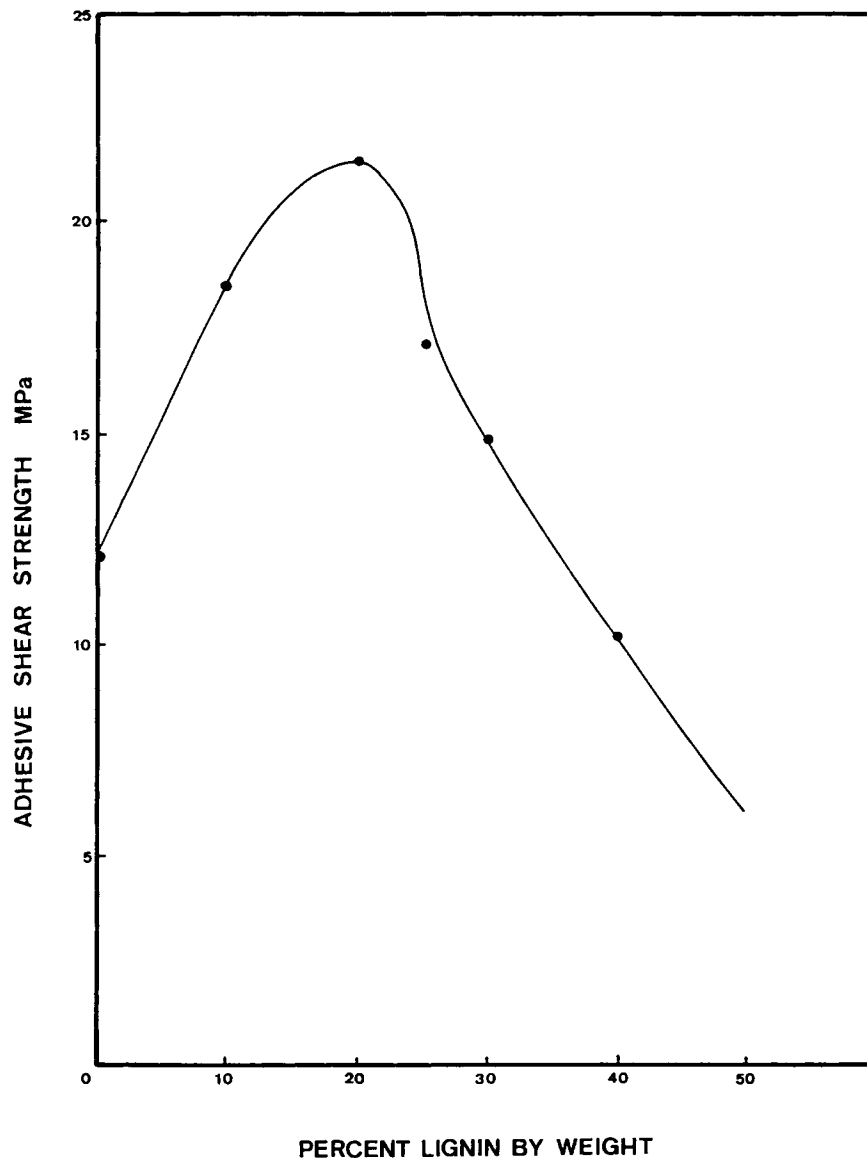
Figure 2 Adhesive shear strength for the EP and EP–L polyblends vs. amount of lignin (curing conditions, 2 h at 100°C).

The results of the adhesive shear strength obtained in these conditions are shown in Figure 3. The storage of EP and EP–20L samples at room temperature prior to the elevated temperature cure caused deterioration of the bond strength in both cases. However, the downtrend is comparable for both EP control and EP–20L as their lap shear strength ratio is constant regardless of the delaying time prior to thermal cure. Similar data were reported by Brett[18] due to delaying the full cure of a DGEBA epoxy prepolymer cured with a polyamine (carried out at temperatures above 80°C). This author correlated the deterioration of the bond

strength with the decrease of the residual exotherm of the respective adhesive, which is in fact a measure of its degree of cure. Based on his DSC results, Brett could conclude that bond failure was cohesive in the range 70–90% cure and became adhesive above 90% cure.

The data from Figure 3 indicate a constant contribution of L to the bond strength in all the cases. This contribution is shown by the ratio of the lap shear strength of EP vs. the lap shear strength of EP–20L, which is constant in the case of both thermally cured specimens as well as for those specimens prepared by delaying time prior to thermal cure.
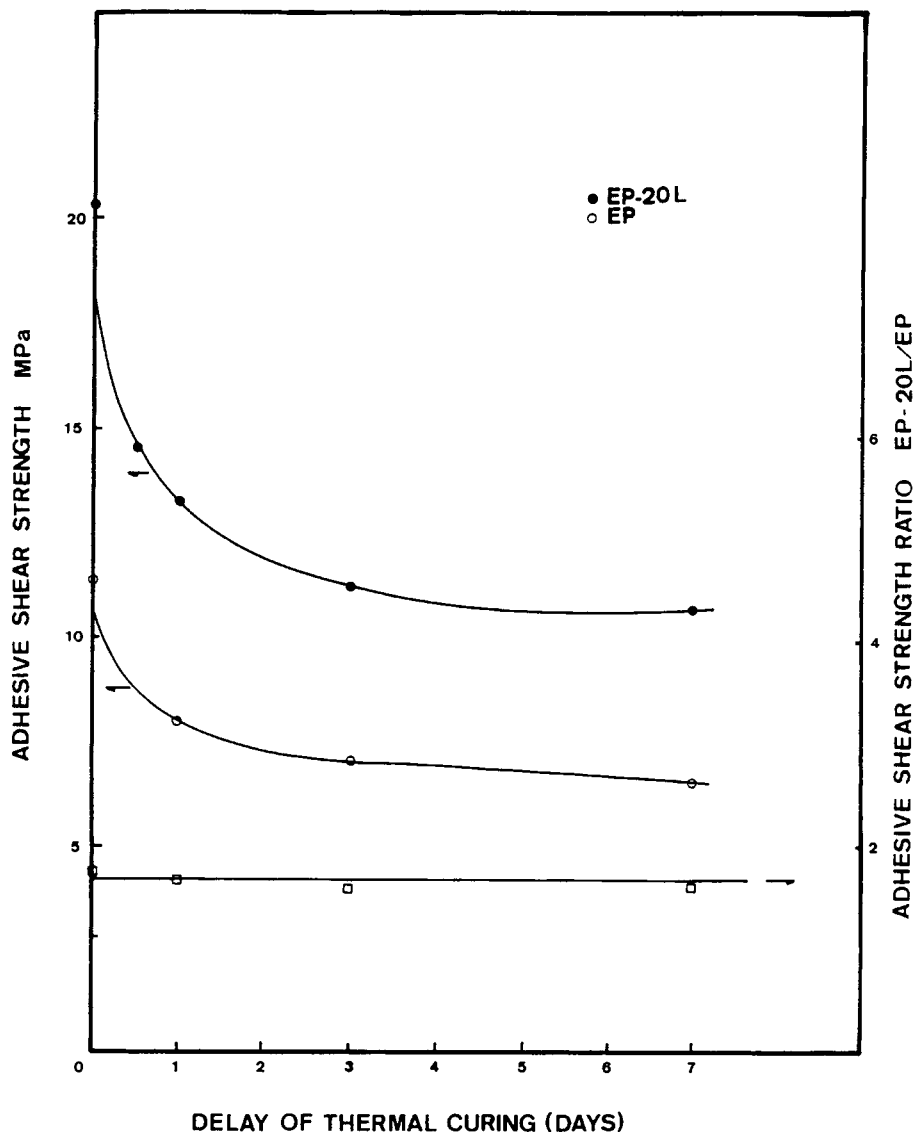
Figure 3 Adhesive shear strength for EP and EP–L20 polyblends vs. delaying of thermal curing.

To further demonstrate the beneficial effects of L on EP polyblends, L was replaced by silica. In a subsequent set of experiments, EP–silica mixtures were prepared, cured, and tested under similar conditions as EP–L polyblends. The EP–20L polyblends, which displayed a maximum lap shear strength in the series 10–40L, also presented higher values than EP–20 silica and even higher than EP–40 silica (Table I).

It has already been shown that the volume fraction of filler and its modulus and strength are those parameters that determine the strength and toughness of the filled epoxy resin. In terms of volume fraction of the filler, the EP–20L polyblends are comparable with EP–40 silica mixture, due to the different specific gravity of L and silica (see "Ma-

terials" section). So at the same volume fraction of filler the bond strength is one and a half times higher for polyblends with L than mixtures with silica, de-

Table I Adhesive Shear Strength of EP, EP–L Polyblends, and EP–Silica Mixtures

Percentage in Mixture			Adhesive Shear Strength (MPa)	
	By Volume			
By Weight	L	Silica	EP–L	EP–Silica
0	0	0	11.40	11.40
20	15.6	7.5	20.26	12.12
40	31.3	15.1	9.61	13.22

1. EP. -0%L 10.38MG.

2. EP. -20%L 9.02MG.

3. EP. -25%L 8.31MG.

4. EP. -40%L 16.68MG.

67.3°C
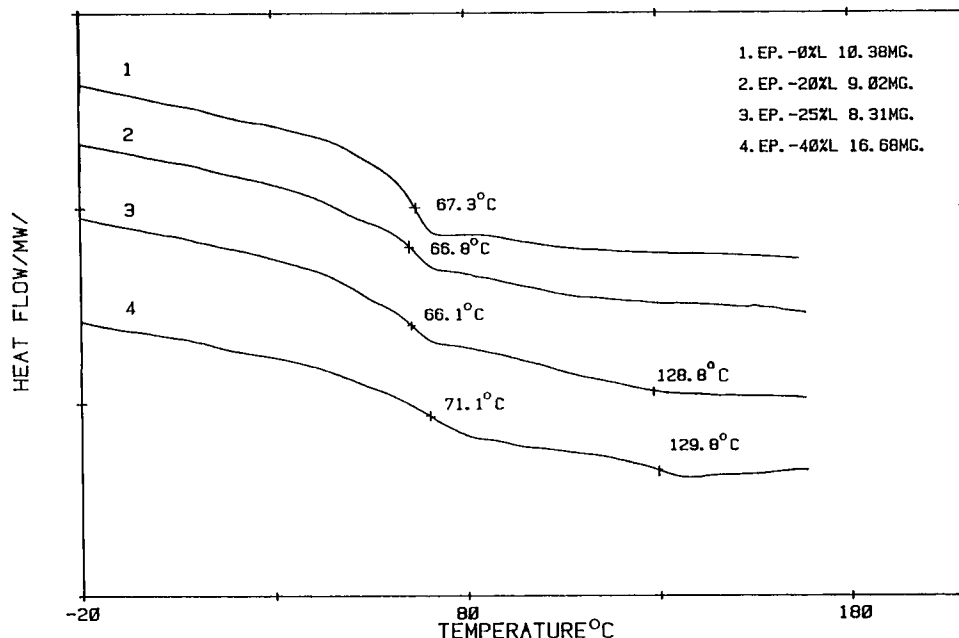
66.8°C

66.1°C

128.8°C

71.1°C

129.8°C

Figure 4   DSC diagrams for EP and EP-L polyblends, run I.

spite the different moduli of L and silica (i.e., 6.6 and 97 GPa, respectively).

A stronger resin–"filler" adhesion is most probably responsible for the higher adhesive shear strength of EP–L polyblends when compared with strengths obtained for EP–silica mixtures. As was suggested in the introduction, this stronger resin "filler" adhesion could be the result of a bond between L and the EP network via certain unreacted amine groups.

DSC

The DSC runs were performed from −40 to 180°C. Preliminary tests with EP or EP–40L were started at −140°C in order to establish the secondary subglass transition, or β transition, which occurs at ca. −60 to −30°C; this is attributable to the crankshaft-type rotation of the epoxy [$-CH_2-CH(OH)-$

CH_2-O-] crosslinking segment.[19,20] We could not locate the β transition for either EP or EP–L specimens. The size of this transition also reflects the curing agent used.[19] It is probable that with the specific type of hardener used, an accelerated aliphatic polyamine, this type of transition is difficult to establish by DSC.

Figure 4 shows the DSC diagrams for EP and EP–L polyblends, as they were obtained in the first run. It can be seen that they do not present any residual exotherm, and consequently, the cure appears to be complete. However, it seems that a further light degree of postcure occurred during the first DSC scans, since the values of T_g's are slightly higher in the second ones.

The differences in T_g's as determined in the first and second runs increase with the L content in EP–L polyblends up to 25% L. This difference might be attributed to some different degree of postcure taking place in the first DSC scans (Table II).

Table II T_g's Values for EP, L, and EP–L Polyblends Determined by DSC and DMA

Lignin Content (%)	First T_g (°C) DSC		ΔT_g (°C) from Run II and Run I	Second T_g (°C) DSC from Run II	T_g DMA (°C) max, tanδ	
	Run I	Run II			First T_g	Second T_g
0	67.3	69.0	1.7	—	78.9	—
20	66.8	70.3	3.5	—	79.7	—
25	66.1	70.8	4.7	129.2	—	—
40	71.1	72.8	1.7	130.3	87.8	146.1
100	—	129–135°	—	—	—	—

The EP-20L polyblend also presents only one T_g located in the region of the T_g's of EP. For EP-25L and EP-40L, a typical heat capacity jump belonging to L is visible and is quite well defined at 129.2 and 130.3°C, respectively (Table II and Fig. 4). It is a clear indication of the immiscibility of L in these polyblends.

DMA

As described earlier, two types of samples were tested by DMA. The first ones, previously cured, were mounted between vertical clamps for quantitative results with respect to modulus, loss modulus, and tanδ. All the measurements, except those for EP, were carried out in a temperature interval of 20–180°C, so that the highest transition interval, as well as the glassy and rubbery state, could be detected.

Tanδ curves for EP and EP-20 and 40L polyblends are shown in Figure 5, and tensile storage modulus curves for the same specimens are shown in Figure 6.

Before discussing the differences in the mechanical relaxation of EP and EP-L polyblends, it is useful to briefly review the concepts concerning the morphology of crosslinked epoxy polymer systems. Several instrumental measurement techniques of epoxy networks have produced ample experimental evidence for the existence of inhomogeneities in their morphology.[20-22] It has been suggested[20-22] that crosslinked epoxy resins consist of highly crosslinked nodules immersed in an internodular matrix of lower crosslink density. According to Mijovic and Tsay,[20] the formation of nodules commences at random spots in the resin-curing agent mixture, as shown in Figure 7.

The elastic storage modulus in the glassy state is determined primarily by the internodular matrix, whereas the onset of molecular motion, corresponding to the glass transition, depends mostly upon the intranodular crosslink densities. This has been demonstrated experimentally by curing EP with stoichiometric and nonstoichiometric amounts of amine-curing agent. An increase in curing agent concentration, up to the stoichiometric ratio, leads to the formation of smaller nodules of higher crosslink density at the expense of the relatively weaker matrix. Mijovic[20] proposes a simplified schematic presentation (Fig. 8) of a relative variation in the moduli of nodules and matrix as a function of the curing agent concentration, which was confirmed by electron microscopy.
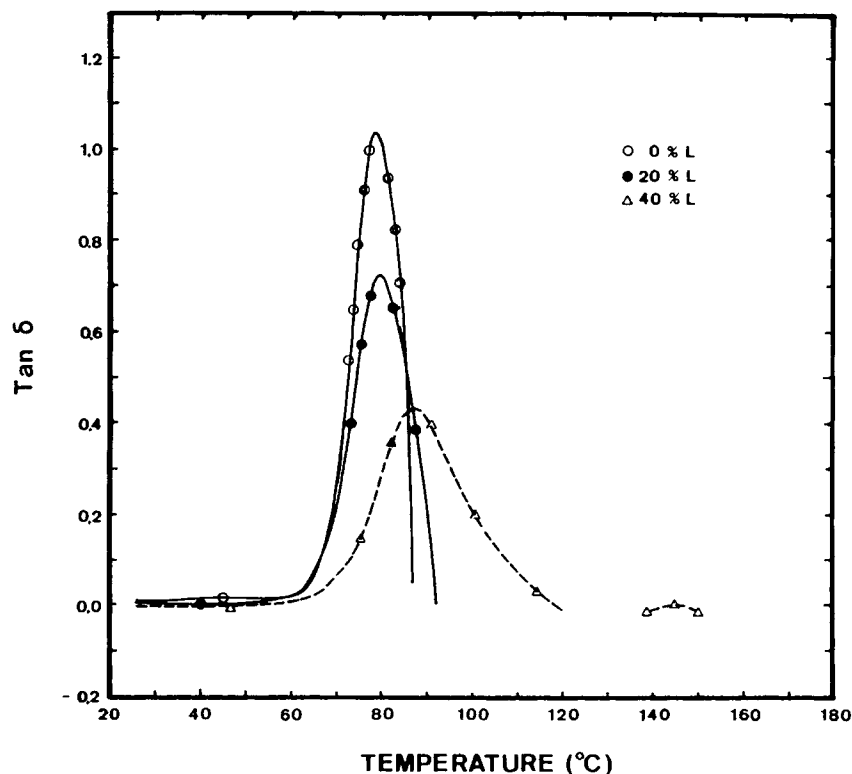

Figure 5   tanδ vs. temperature for EP, EP-L polyblends: specimens mounted in vertical mode; heating rate, 5°C/min.
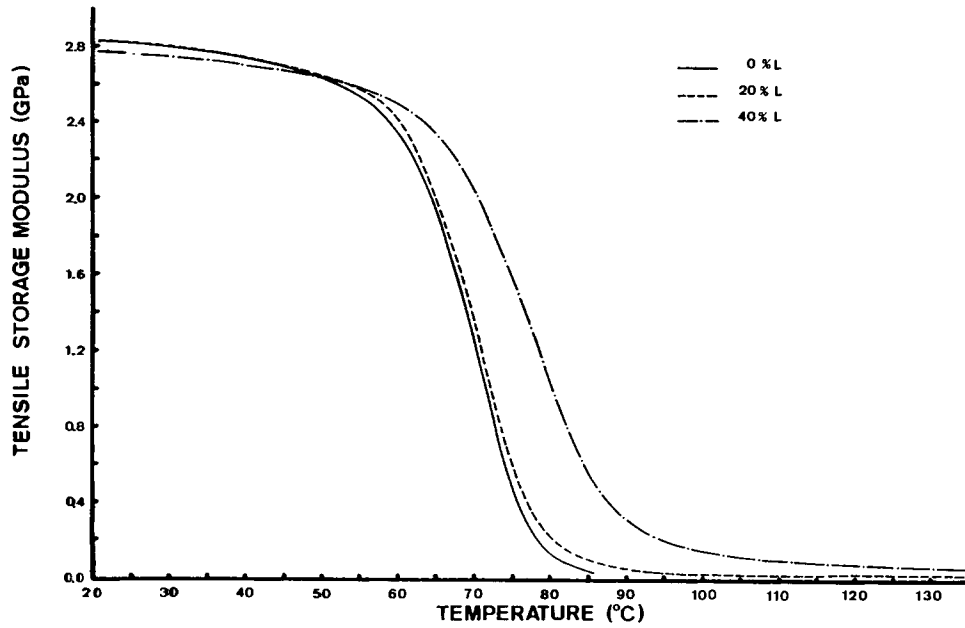
Figure 6   Tensile storage moduli vs. temperature for EP and EP–L polyblends: specimens mounted in vertical mode; heating rate, 5°C/min.

It should first be noted from observation of the tanδ curves (Fig. 5) that the transition region from the glasslike to the rubberlike state shifts slightly to higher temperature only in the case of EP–40L. The glass transition region covers a broader temperature range, i.e., from 60 to 95°C for EP–20L and
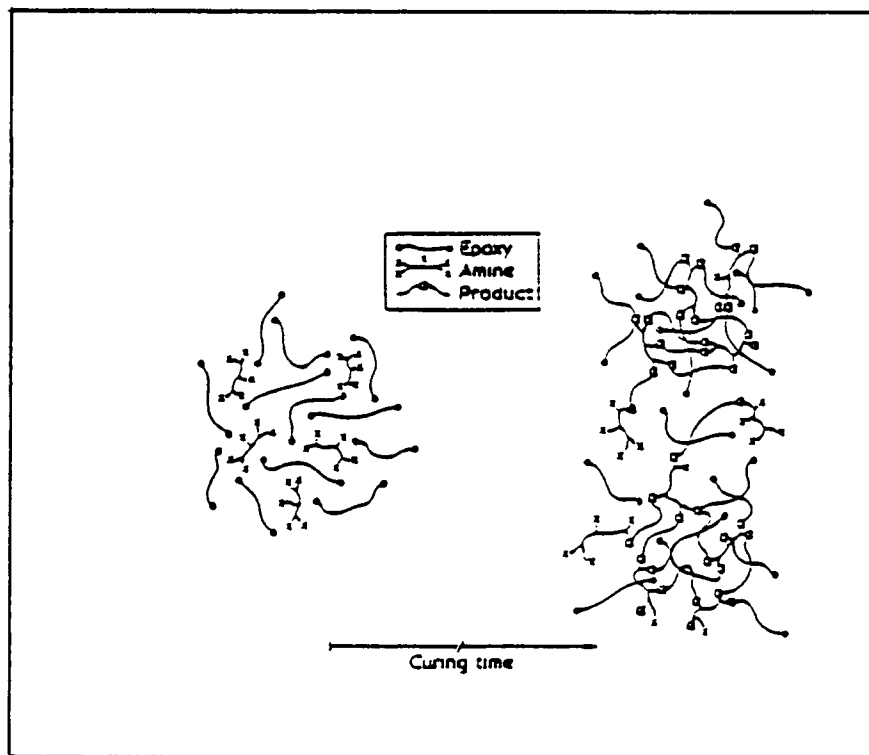

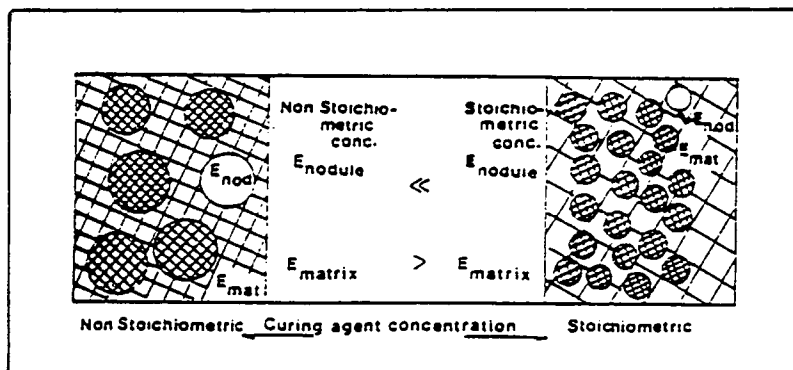**Figure 7**   Schematic presentation of initial formation of nodules in the EP resin curing agent mixture.[20]

Figure 8 Schematic presentation of variations in moduli of nodules and matrix as a function of a curing agent concentration.[20]

from 60 to 120°C for EP–40L. This compares with a transition region from 60 to 88°C for EP.

The broadening of the tanδ peak is probably due to the traces of L bonded to the epoxy network as a result of its reaction with free amine groups present in the hardener. The presence of L will reduce the motion of those nodules to which it is bonded. As a consequence of this immobilization, the glass transition is extended toward higher temperatures. As was mentioned earlier, the bonding of L to the epoxy network, in the case of EP–20L polyblends, can create a stronger resin–"filler" adhesion. This enhanced resin–L adhesion would be responsible for the higher bond strength of EP–20L polyblends when compared with EP or even with EP–40 silica mixtures. However, if a higher quantity of L is bonded to the final epoxy network, as in the case of EP–40L polyblends, the bond strength is drastically reduced.

The T_g may also be evaluated from temperature readings at peak values of tanδ. The results, although quite close, follow the same trend as determined for T_g's evaluated using DSC (Table II and Fig. 4).

Examination of the tensile storage moduli in Figure 6 shows that at room temperature the storage moduli are influenced very little by the presence of L. As mentioned earlier, the storage modulus in the glassy state is determined primarily by the weak internodular matrix. In increasing the L content from zero to 40%, it is seen that all polyblends display nearly the same storage modulus but slightly higher glass transition temperatures. It looks likely that the internodular matrix is unchanged and that some changes occurred only in the intranodular one due to presence of L.

It can also be seen from the tanδ curves that the components of EP–20L polyblends are miscible since they exhibit a single T_g characteristic of a monophasic system.[23] For EP–40L polyblends, a second peak in the tanδ curve, although barely detectable, is located in the temperature region characteristic for L molecular motions and this, in form, discloses the immiscibility of these polyblends.

Similar results concerning the miscibility of EP–20L and the immiscibility of EP–40L polyblends were also obtained from DSC analysis (Table II and Fig. 4).

In another set of DMA tests, uncured EP or EP–L polyblends were placed on strips of fiberglass cloth previously mounted between horizontal clamps.

In DMA, the deformation in the horizontal mode is a complex process, involving shearing, bending, and compressive forces such that quantitative moduli cannot be obtained.[12] However, our intention was to follow the progress of the curing process from changes in frequency and damping signals and hence to confirm whether or not the two polymers were miscible. As can be seen from Figure 5, the tanδ values for the second T_g were very low and below the detection limits of the instrument.

A set of dynamic tests was performed between 20 and 180°C at a heating rate of 5°C/min such that the contact time between EP in the rubbery state and L was small. As can be seen from the right side of the damping-vs.-temperature curves (Fig. 9), the damping signals reach a maximum at ca. 106°C after which they drop off rapidly. The drop is continuous for EP, but for EP–L polyblends a second damping signal peak appears at ca. 150°C due to L motions from the glassy to the rubbery state. The height of the second damping peak for EP–L polyblends can easily be correlated with the L content in each polyblend. It appears that almost all of the L present in polyblends is free, since its presence does not change the maximum peak position of the first damping signal, which itself is associated with EP motions.
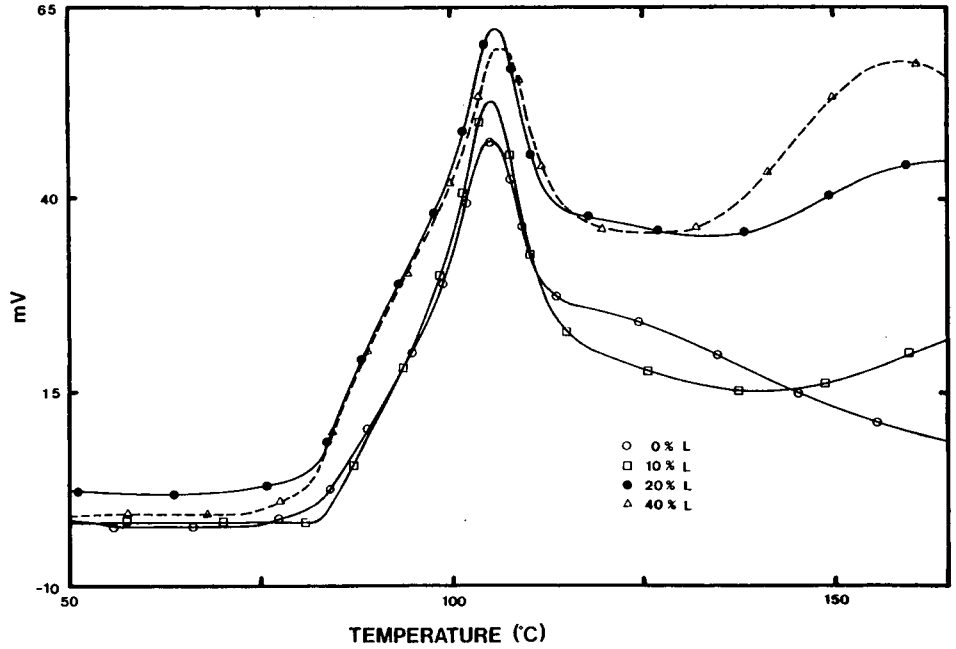
Figure 9 DMA damping signals vs. temperature during the curing process for EP and EP–L polyblends: specimens mounted in horizontal mode; heating rate, 5°C/min.

The presence of a second damping peak that correlates with the glass transition of L indicates the immiscibility of L in all the polyblends at a short contact time between EP in the rubbery state and L.

In another set of tests, the same type of samples were first isothermally cured in the DMA oven at 100°C for 2 h. These were the same conditions as for the thermal cure of the EP and polyblends. After 2 h the samples were allowed to cool to room tem-
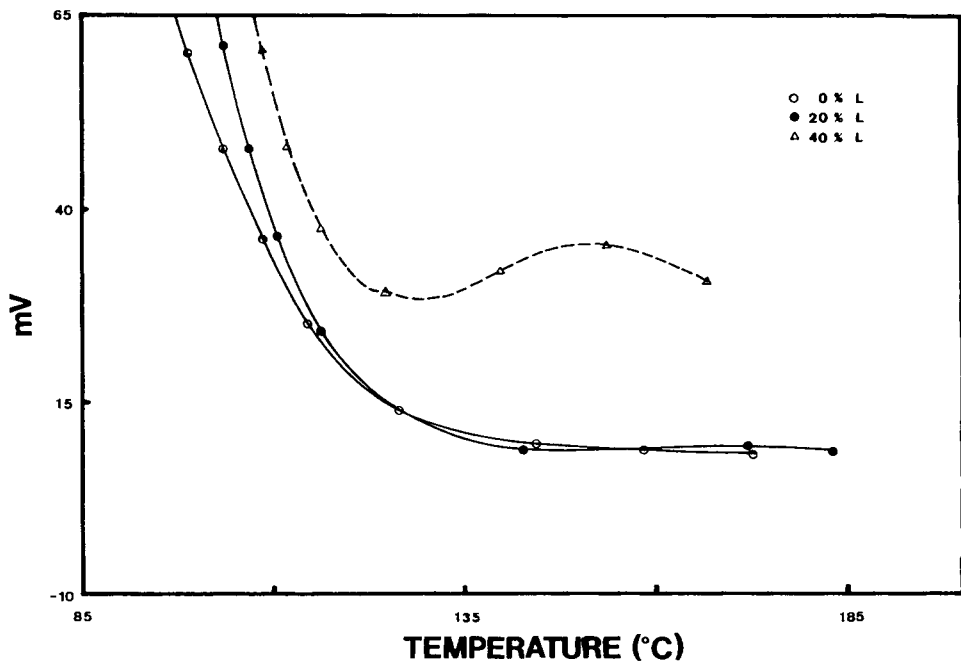

Figure 10 DMA damping signals vs. temperature for EP and EP–L polyblends previously isothermally cured for 2 h at 100°C: specimens mounted in horizontal mode; heating rate, 5°C/min.

perature for 2 h and were then tested again. The damping signals in the L glass transition region were plotted at the same scale as for the previous dynamic experiments (Fig. 9) and are illustrated in Figure 10. In this instance, in the damping signals for EP and EP–20L the second damping peak due to L's T_g is not identifiable. However, for the EP–40L polyblend, a second damping signal peak appears due to L motions, thus indicating the immiscibility of L.

NMR Spectra

The high-resolution solid-state NMR spectra were obtained on a Bruker CXP-200 spectrometer with a Doty probe. The measurements were performed at room temperature under magic angle spinning at ca. 2.5 KHz using a cross-polarization field that generated a proton 90° pulse of 3.7 μs. The repetition delay was set at 10 s, and the contact time was varied as long as signal was being obtained. From the graphs of ln (signal intensity) as a function of contact time, the rotating frame parameter ($T_1\rho H$) was calculated. This parameter was suggested as a probe of phase composition for blends in 1981[24] and has since then been used in various systems. It was previously used by us for blends of a polyurethane with L.[25]

The CP-MAS NMR spectrum of L was previously assigned[26] and has the most important signals at 56 ppm (the aromatic methoxy carbons) and at 149 ppm (the aromatic ring carbons 3 and 4). The $T_1\rho H$ of all lignin signals in the conditions mentioned in the preceding is 16.5 ms. The EP–control, as well as all polyblends analyzed here, has a rather complicated spectrum due to many spinning side bands. Unlike L, which is a powder and can be easily packed into the spinner, all other samples had to be cut into

pieces to fit the spinner. This created inhomogeneities in the sample distribution, hence the appearance of the spinning side bands. Figure 11 presents a spectrum of thermally cured EP–control sample. The only assignable signals are in the region of 20–40 ppm (aliphatic carbons) and 60–70 ppm (carbons neighboring oxygen). There are some (or only one) carbonyl signals, but it is impossible to say which are (is) or are not real. The $T_1\rho H$ for the EP–control is 3.7 ms.

Two $T_1\rho H$ values are found to occur in each set of polyblends corresponding to two phases. The two values can be obtained from the signals belonging to the EP–control and to the L, respectively. Consequently, it is reasonable to assume that no molecular mixing takes place. However, as can be seen in Figure 12, the two $T_1\rho H$ values are not constant over the whole composition range. The $T_1\rho H$ of the L decreases with a corresponding decrease of L in the blend. The $T_1\rho H$ of the epoxy part, however, seems to increase for a 20% composition in the blend and then decrease to the initial value. At this 20% composition, the lignin $T_1\rho H$ is almost as low as the epoxy $T_1\rho H$, making the blend seem homogeneous, even by NMR standards.

Due to the poor resolution, it is difficult to explain if there are chemical reactions taking place and to what extent. However, from the shape of the curves in Figure 12, it seems reasonable to assume that a stoichiometric reaction occurs at 20% L. The extent of the reaction is probably never sufficient as to mix the two components of the blend to the molecular level, but it is the highest at this composition, generating homogeneous properties on the macroscale and creating the appearance of a homogeneous mixture even on a very fine scale (a few angstroms, as observed by NMR).
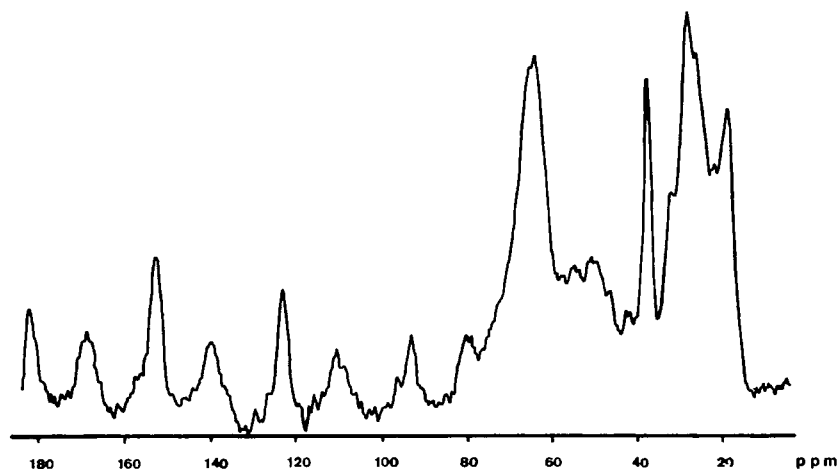

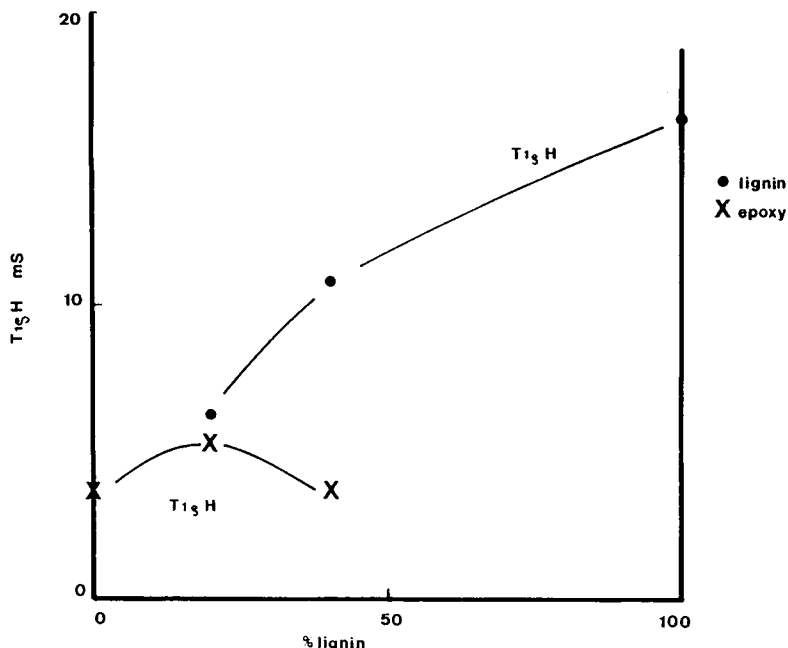**Figure 11** CP-MAS NMR spectra of thermally cured EP control sample.

Figure 12 $T_1\rho H$ signal for EP and L in control specimens and EP–L polyblends.

DISCUSSION AND CONCLUSION

A systematic investigation was conducted for thermally cured EP–L polyblends having up to 40% L content. Adhesive shear tests, DSC, DMA, and solid-state CP-MAS NMR spectra were performed to establish the effect of L on the mechanical properties of the polyblends and on the morphology of these crosslinked structures.

The adhesive shear test in tension disclosed a considerable improvement in adhesion in blends having up to 30% L content with a maxima occurring at a 20% L loading. However, the shear strength is drastically reduced in specimens of blends having L contents in excess of 35%.

At the same volume fraction of filler the bond strength was one and a half times higher for EP–20L blends than for control EP–40 silica blends despite their very different modulus.

The T_g's of the EP–L polyblends were within proximity of one another with a slight trend to increasing both in DSC and DMA analyses, mostly for EP–40L. Only one T_g was detected for blends having up to 20% L content but two T_g's for blends having higher L contents. Hence, the EP–L blends are miscible up to L contents of 20%.

The tanδ peak broadened with higher L content whereas all the EP and EP–L DMA moduli were very nearly similar.
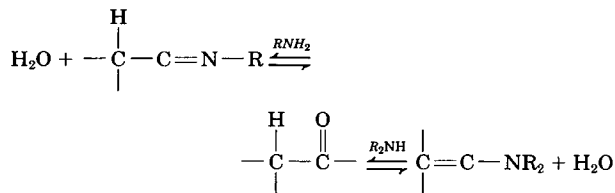
Curing studies performed using the DMA scanning mode showed a damping maximum at 106°C

for EP and all EP–L blends, whereas a second damping peak was present at ca. 130°C for all EP–L blends but not for EP. It was also found that with the exception of the EP–40L blend precuring of the blends at 100° for 2 h leads to the disappearance of the second damping peak.

From the shape of the proton spin–lattice relaxation time curves, (calculated from solid-state NMR spectra) showing $T_1\rho H$ as a function of L content, it seems reasonable to assume that a stoichiometric reaction occurred at a blend loading of 20% L. The extent of the reaction was probably not sufficient for the two components to combine at the molecular level, but it was significant enough to generate homogeneous properties on the macromolecular scale. This was disclosed from the results of DSC and DMA measurements.

A reasonable explanation for the different behavior of EP–L polyblends as a function of their L content could be the enhanced degree of bonding between L and the EP network taking place at elevated temperatures. This bonding can arise by a chemical reaction between L and some unreacted amine groups present in the hardener. A possible lignin–amine reaction was postulated in an earlier work based on the curing kinetics evaluated using the DSC technique.

The carbonyl groups present in L, in a proportion of about 5%, seem to be the most susceptible groups to react with amines (secondary or primary) according to the following reactions:

$$H_2O + \ -\overset{\overset{\displaystyle H}{|}}{\underset{|}{C}}-C{=}N-R \overset{RNH_2}{\rightleftharpoons}$$

$$-\overset{\overset{\displaystyle H}{|}}{\underset{|}{C}}-\overset{\overset{\displaystyle O}{\|}}{C}-\overset{R_2NH}{\rightleftharpoons} \overset{\overset{\displaystyle |}{}}{\underset{|}{C}}{=}C-NR_2 + H_2O$$

These reactions are acid catalyzed, having a very slow reaction rate at either high or low pH.[27]

It seems that L–amine reaction does not really compete with the principal addition reactions of epoxide groups with primary and secondary amines, at least in those blends having no greater than 20% L. The T_g of EP–L blends, with the exception of the EP–40L blend, did not show any amine–epoxy unbalance.

For explaining the very close value of DMA moduli at room temperature for EP and EP–L polyblends without an amine–epoxy unbalance, the concept of nodular morphology of crosslinked epoxy resins was applied. Similarity in DMA moduli was explained by an unchanged internodular matrix. The bonding of L was supposed to occur almost in the intranodular matrix, and it is also responsible for the broadening of tanδ peak curves.

Curing studies performed using the DMA scanning mode have shown that L–amine reactions take place only at elevated temperatures and a contact time not less than 1 h.

It appears likely that blends having 20% L provided the ideal conditions for a "stoichiometric" reaction involving L carbonyl groups and the unreacted amine groups present in the hardener. Of those polyblends evaluated in this study, polyblends having 20% L content were found to possess the greatest degree of adhesion and, as well, the most complete miscibility as evaluated by thermal analysis techniques.

REFERENCES

1. P. O. Nielsen, *Adhesive Age*, April, 42–46 (1982).
2. D. Feldman and D. Banu, *J. Polym. Sci., Chem. Ed.*, **26**, 973–983 (1988).
3. D. Feldman and M. Khoury, *J. Adhesion Sci. Technol.*, **2**(2), 107–116 (1988).
4. D. Feldman, D. Banu, and M. Khoury, *J. Appl. Polym. Sci.*, **37**, 877–887 (1989).
5. W. G. Glasser and S. S. Kelley, in *Encylopedia of Polymer Science and Engineering*, Kroschwtiz, J. (Ed.) Wiley, New York, 1984, Vol. 8. p. 795.
6. N. Shiraishi, H. Ito, and N. Tsujimoto, JP 61,215,678 (86, 215, 678) through *Chem. Abstr.*, **106**, 85296 m (1987).
7. N. Shiraishi, in *Lignin Properties and Materials*, W. G. Glasser and S. Sarkanen (Eds.), ACS Symposium Series 397, American Chemical Society, Washington, D.C., 1989, pp. 488–495.
8. B. Tomita, A. Kurozumi, and S. Hosoya, in *Lignin Properties and Materials*, W. G. Glasser and S. Sarkanen (Eds.), ACS Symposium Series 397, American Chemical Society, Washington, D.C., 1989, pp. 496–505.
9. W. L. S. Nieh and W. G. Glasser, in *Lignin Properties and Materials*, W. G. Glasser and S. Sarkanen (Eds.), ACS Symposium Series 397, American Chemical Society, Washington, D.C., 1989, pp. 506–513.
10. F. T. Ball, W. K. Doughty, and H. H. Moorer, Canadian Pat. 654,728 (1962).
11. H. Lee and K. Neville, *Handbook of Epoxy Resins*, McGraw-Hill, New York, 1967.
12. R. B. Prime, "Thermosets" in E. A. Turi (Ed.), *Thermal Characterization of Polymeric Materials*, Academic Press, New York, 1981, pp. 435–569.
13. Y. Tanaka and T. F. Mika, "Epoxide Curing Reaction," in *Epoxy Resins—Chemistry and Technology*, C. A. May and Y. Tanaka (Eds.), Marcel Decker, New York, 1973, pp. 135–238.
14. R. J. Morgan, F. M. Wong, and C. M. Walkup, *Polymer*, **25**, 375–386 (1984).
15. W. Cousins, *J. For. Sci.*, **7**(1), 107 (1977).
16. A. C. Moloney, H. H. Kausch, and H. R. Stieger, *J. Mater Sci.*, **18**, 208–216 (1983).
17. A. C. Moloney, H. H. Kausch, T. Kaiser, and H. R. Beer, *J. Mater Sci.*, **22**, 381–393 (1987).
18. C. L. Brett, in *Adhesion*, W. E. Allen (Ed.), Applied Science Publishers, London, 1979 Vol. 3, pp. 53–64.
19. J. H. Kaelble, "Properties of Cured Resins," in *Epoxy Resins—Chemistry and Technology*, C. A. May and Y. Tanaka (Eds.), Marcel Decker, New York, 1973, pp. 342–343.
20. J. Mijovic and L. Tsay, *Polymer*, **22**, 902–906 (1981).
21. J. E. Kantou, G. Spathis, and P. Theocaris, *J. Polym. Sci., Polym. Chem. Ed.*, **23**, 1493–1503 (1985).
22. J. Mijovic and King-Fu Lin, *J. Appl. Polym. Sci.*, **32**, 3211–3227 (1986).
23. O. Olabisi, L. M. Robeson, and M. T. Shaw, *Polymer-Polymer Miscibility*, Academic Press, New York, 1979.
24. J. Schaefer, M. D. Sefcik, E. O. Stejskal, and R. A. McKay, *Macromolecules*, **14**, 275 (1981).
25. A. Natansohn, M. Lacasse, D. Banu, and D. Feldman, *J. Appl. Polym. Sci.*, **40**, 899–904 (1990).
26. W. Kolodziejski, J. S. Frye, and G. E. Maciel, *Anal. Chem.*, **54**, 1419 (1982).
27. J. McMurry, *Organic Chemistry*, Sec. Ed., Brooks/Cole, 1988, pp. 674–675, 910–911. Monterey, CA.